Published in final edited form as:
J Cell Biochem. 2013 April ; 114(4): 782–795. doi:10.1002/jcb.24416.

Actin realignment and cofilin regulation are essential for barrier integrity during shear stress

Joshua B. Slee[1] and **Linda J. Lowe-Krentz**[1,*]

[1]Department of Biological Sciences Lehigh University, Bethlehem, PA 18015

Abstract

Vascular endothelial cells and their actin microfilaments align in the direction of fluid shear stress (FSS) in vitro and in vivo. To determine whether cofilin, an actin severing protein, is required in this process, the levels of phospho-cofilin (serine-3) were evaluated in cells exposed to FSS. Phospho-cofilin levels decreased in the cytoplasm and increased in the nucleus during FSS exposure. This was accompanied by increased nuclear staining for activated LIMK, a cofilin kinase. Blocking stress kinases JNK and p38, known to play roles in actin realignment during FSS, decreased cofilin phosphorylation under static conditions, and JNK inhibition also resulted in decreased phospho-cofilin during FSS exposure. Inhibition of dynamic changes in cofilin phosphorylation through cofilin mutants decreased correct actin realignment. The mutants also decreased barrier integrity as did inhibition of the stress kinases. These results identify the importance of cofilin in the process of actin alignment and the requirement for actin realignment in endothelial barrier integrity during FSS.

Keywords

Vascular endothelial cells; Fluid shear stress; Actin realignment; Cofilin; Barrier integrity

Fluid shear stress (FSS) plays important roles in embryonic morphogenesis of the vasculature, regulation of vessel diameter in adulthood, maintaining vascular homeostasis, and is implicated in the development of atherosclerosis (reviewed in Hahn and Schwartz, 2009). Vascular endothelial cells (ECs) respond to sustained laminar FSS by increasing their antithrombic activity, decreasing reactive oxygen species, increasing antioxidant enzymes, and altering growth factor signaling (reviewed in Yamamoto and Ando, 2011). It has been estimated that more than 600 EC genes respond to FSS (Ohura et al., 2003). FSS has been shown to activate a variety of signaling pathways in ECs, but it is still unclear how the cell initially senses this mechanical stress. The signaling pathways which have been shown to be activated by FSS include: ion channels leading to Ca^{2+} influx, tyrosine kinase receptors leading to JNK activation, G-protein coupled receptors, and various adhesion proteins (reviewed in Yamamoto and Ando, 2011).

Correspondence: Linda J. Lowe-Krentz, 111 Research Drive, Bethlehem, PA 18018, Lehigh University, Phone: 610-758-5078, Fax: 610-758-4004, ljl0@lehigh.edu.

There have been recent advances in understanding the mechanotransduction induced by FSS, such as, the importance of cell-cell junctions (Tzima et al., 2005) and involvement of the actin cytoskeleton (Osborn et al., 2006). It is becoming clear that at least one mechanosensing mechanism involves a complex of PECAM-1 (platelet endothelial cell adhesion molecule-1), VE-cadherin (vascular-endothelial cadherin), and VEGFR2 (vascular endothelial growth factor receptor 2) (reviewed in: Conway and Schwartz, 2012). Within this complex, PECAM-1 and VEGFR2 are responsible for downstream signaling, while VE-cadherin functions as an adaptor (Tzima et al., 2005). VE-cadherin is an endothelial cell specific component of adherens junctions and is essential for maintaining endothelial barrier integrity (Vincent et al., 2004). The cytoplasmic domain of VE-cadherin associates with p120-, β-, γ-, and α-catenin in endothelial cell-cell junctions to mediate downstream signaling (Dejana et al., 2008), with VE-cadherin connecting to the actin cytoskeleton via β-catenin (Tharakan et al., 2012). Given the importance of the endothelial barrier for vascular permeability, it is imperative that the endothelial barrier remain intact during FSS. ECs exposed to FSS exhibit a marked increase in transendothelial resistance, illustrating a strengthening of the barrier compared to static cells (DePaola et al., 2001, Seebach et al., 2000). Given that the VE-cadherin/β-catenin adhesions are linked to actin, we predicted that disruptions to the actin realignment process during FSS would disrupt endothelial barrier integrity.

In vivo and in vitro evidence indicates that laminar FSS (15dynes/cm^2) causes endothelial cell and actin microfilament alignment in the direction of FSS (Mengistu et al., 2011, Kadohama et al., 2006, Noria et al., 2004, Malek and Izumo, 1996), but the molecular mechanisms underlying this remodeling remain unclear. JNK and p38 are critically important during FSS-induced actin realignment. Studies investigating the role of JNK during FSS indicate that the JNK signaling pathway mediates, at least in part, FSS-induced actin realignment (Mengistu et al., 2011, Hahn et al., 2011). It has also been demonstrated that p38 activity is required for complete FSS-induced actin remodeling (Azuma et al., 2001, Mengistu et al., 2012). There is a large amount of data detailing the roles of JNK and p38 in migrating cells during wound healing (Reviewed in: Mengistu et al., 2012), as well as association with cytoskeletal structures in proliferating ECs (Hamel et al., 2006).

Regulation of actin microfilaments depends in part upon the Actin Depolymerizing Factor (ADF)/cofilin family of proteins, of which cofilin-1 is the most prominent in non-muscle tissue (Lin et al., 2010, Suurna et al., 2006, Berstein and Bambrug, 2010). The ADF/Cofilin proteins are expressed in all eukaryotes and can, for the most part, rescue deletions of other family members (Berstein and Bambrug, 2010). However, cofilin-1 cannot be rescued by other family members and knockout is embryonically lethal in mice (Gurniak et al., 2005). One of the major regulatory mechanisms controlling cofilin (from this point forward refers to cofilin-1) activity is phosphorylation at serine-3. Phospho-cofilin (serine-3) (p-cofilin) is dephosphorylated by cofilin phosphatases, including chronophin and the slingshot (SSH) family of protein phosphatases and therefore activated. Once dephosphorylated, cofilin binds to both G-actin and F-actin in a 1:1 molar ratio and promotes F-actin depolymerization (Nishida et al., 1984). Cofilin is inactivated by phosphorylation at serine-3 via the Lin-11/Isl-1/Mec-3 domain-containing protein kinase (LIMK) family, resulting in the formation of

actin stress fibers (Suurna et al., 2006, Won et al., 2009, Keezer et al., 2003, Côté et al., 2010, Bernard O, 2007).

It is becoming clear in the literature that actin is essential not only in the cytoplasm, but also in the nucleus, for regulation of transcription and gene expression (Zheng et al., 2009, Pederson, 2008). Actin alone is incapable of entering the nucleus, as it lacks a nuclear localization sequence, requiring it to associate with other proteins to facilitate nuclear entry. One of the leading hypotheses is that cofilin is responsible for localizing actin to the nucleus (Berstein and Bambrug, 2010, Mengistu et al., 2012). Cofilin has a nuclear localization sequence (KKRKK) similar to that of SV40 large T antigen (Iida et al., 1992, Karderon et al., 1984), and dephosphorylated cofilin has been reported to localize to the nucleus after various cell stresses, such as heat shock, latrunculin B treatment, or ATP depletion (Pendleton et al., 2003, Iida et al., 1992). LIMK-1 possesses two leucine-rich nuclear export signals within its PDZ domain and one NLS-like sequence responsible for nuclear localization (Yang and Mizuno, 1999), suggesting that LIMK-1 could phosphorylate cofilin in the nucleus. Definitive roles for cofilin in the nucleus have yet to be elucidated, but it has been predicted to facilitate nuclear actin depolymerization, as it does in the cytoplasm.

In this study, we exposed vascular ECs to 15dynes/cm^2 FSS to determine the role of cofilin in FSS-induced actin realignment, further our understanding of the role of stress kinases in this process, and assess the effect of FSS-induced actin realignment on EC barrier integrity. Our results indicate that FSS induces accumulation of p-cofilin in the nucleus, likely phosphorylated by pLIMK1/2, whose activity in the nucleus is also responsive to FSS. Our results indicate that proper FSS-induced regulation of cofilin and actin are essential for FSS-induced realignment and barrier maintenance and enhancement.

Materials and Methods

Cell Culture

Bovine aortic endothelial cells (BAECs) were obtained from Cell Applications (San Diego, CA) and cultured using Cell Applications BAEC media according to their recommendations. BAECs were cultured onto 30 mm diameter, 0.17 mm thick glass cover slips coated with 30 μg/ml bovine collagen type I (BD, San Jose, CA) in phosphate-buffered saline, placed in six-well culture plates, and grown for approximately 18 hours until they formed a confluent monolayer. BAECs were incubated for 1 hr in shear media (MEM containing HEPES (Sigma-Aldrich, St. Louis, MO), supplemented with 0.5% heat-inactivated FBS (Biowest, Miami, FL or Invitrogen, Grand Island, NY)) prior to shear exposure to maintain pH and to minimize bubble formation. The cover slips were assembled into a modified POC-mini-plate flow chamber (Yalcin et al., 2007) for exposure to FSS conditions. Typically, BAECs between passages 5 and 20 were used for these experiments.

JNK and p38 Inhibitor Treatments

JNK activity was inhibited using SP600125 (Calbiochem-EMD Millipore Chemicals, Billerica, MA), a competitive inhibitor for JNK (Bogoyevitch et al., 2004). p38 activity was inhibited using SB203580 (Calbiochem) which binds to the ATP-binding pocket inhibiting

its catalytic activity, but not p38 phosphorylation (Kumar et al., 1999). BAECs were cultured as described above and were then incubated with 10μM of either the JNK or the p38 inhibitor in shear media for 1 hour prior to FSS exposure. FSS exposure was carried out as described below.

FSS Experiments

A POC mini chamber from Hemogenix (Colorado Springs, CO) was modified by adding a gasket with a rectangular flow channel to create an adjustable-height parallel-plate flow chamber as previously described (Yalcin et al., 2007). FSS was calculated using the following equation: $\tau_w = \frac{6\mu Q}{WH^2}$ where τ_w is the wall shear stress, μ is the viscosity (0.007 dynes/cm^2 at 37 °C), Q is the flow speed, and W and H are the width and height of the gasket, respectively. BAECs were exposed to 15 dynes/cm^2 shear stress (τ_w) according to the following parameters: W = 1 cm, H = 0.01 cm and Q = 2.14 ml/min. A constant flow of shear media was supplied to the POC mini parallel-plate flow chamber using a REGLO Digital continuous flow pump from ISMATEC International (IDEX Health & Science, Wertheim-Mondfeld, Germany). The FSS experiments were carried out at 37 °C.

Immunofluorescence Staining

After inhibitor treatment (where applicable) and FSS exposure, BAECs were washed with PBS, fixed, and permeabilized with ice-cold methanol for 5 mins at −20 °C and washed again with PBS. The cover slips were incubated with primary antibodies against p-Cofilin (serine-3), pLIMK1/2 (threonine-508/505), VE-cadherin, β-catenin (Santa Cruz Biotechnology, Santa Cruz, CA), total Cofilin (Santa Cruz Biotechnology and Cell Signaling, Boston, MA), pLIMK (serine-323), or pSSH (serine-978) (ECM Biosciences, Versailles, KY), overnight at 4 °C. Cells were then washed with PBS and incubated with secondary antibodies conjugated to FITC or TRITC (Jackson ImmunoResearch, West Grove, PA) overnight at 4 °C. Both primary and secondary antibodies were used at dilutions recommended by the suppliers. Cover slips were mounted in mowoil (Calbiochem) to minimize photobleaching.

In experiments in which actin stress fibers were detected, TRITC-phalloidin (Sigma-Aldrich, St. Louis, MO) was used. For these samples, the cells were fixed with 2.0% formaldehyde (Sigma-Aldrich) and permeabilized with 0.2% Triton-X-100 (Sigma-Aldrich). In some cases, this fixation method was used as an alternative to confirm patterns seen with methanol fixation. Cover slips were washed with PBS and incubated with TRITC-phalloidin at the supplier's recommended dilution overnight at 4°C. Following incubation, cover slips were mounted as described above.

Cofilin Mutant Transfection Protocol

A constitutively active, phosphorylation defective cofilin (serine-3-alanine – S3A), mutant construct and a constitutively inactive, phosphomimic cofilin (serine-3-aspartic acid – S3D), mutant were used (Mutants provided by Theo Rein, Max Planck Institute of Psychiatry, Müchen, Germany) (Rüegg et al., 2004). BAECs were electroporated with 20 μg/ml of one cofilin construct and GFP-vinculin (GFP-vinc - provided by Kenneth Yamada, National

Institute of Dental and Craniofacial Research, Bethesda, MD) as a fluorescent control using the Bio-Rad Gene Pulser X-Cell System (Hercules, CA) and the manufacturer's recommended protocol modified to achieve a confluent monolayer of BAECs. Briefly, 100 mm confluent plates of cells were trypsinized, rinsed with PBS, suspended in HEPES-buffered saline, electroporated, and re-plated. Once confluent, the cells were split onto glass cover slips as described above, grown to confluency (approximately 18 hrs), and exposed to FSS as described above. GFP-vinc is readily taken up and expressed by BAECs, but in our experiments did not associate appreciably with focal adhesions in the time between seeding and FSS experiments. Transfection efficiencies close to 100% were consistently obtained based on GFP-vinc transfection.

SDS-polyacrylamide gel electrophoresis (SDS-PAGE) and Western Blotting

Confluent BAECs expressing GFP-vinc, S3A cofilin, or S3D cofilin were lysed with SDS sample buffer as previously described (Hamel et al. 2006). Proteins were resolved by SDS-PAGE and electrophoretically transferred onto nitrocellulose and blots were probed with antibodies for p-cofilin or total-cofilin and secondary antibodies conjugated to biotin (Jackson ImmunoResearch). Blots were developed using ExtraAvidin™ alkaline phosphatase, BCIP, and NBT (Sigma). Bands of interested were identified by comparison with lanes using only secondary antibodies and by molecular weight based on migration of pre-stained Rainbow™ molecular weight markers (GE Healthcare Biosciences, Piscataway, NJ). Rf values for the molecular weight markers were used to generate a standard curve which was used to calculate the molecular weight of the bands of interest. Acylamide solutions were obtained from Amresco (Solon, OH).

Confocal Microscopy

Fluorescent labels were visualized using the Zeiss© LSM 510 Meta with a 63X oil-immersion lens at room temperature. All images were taken at approximately the same Z-plane of the cell where intensity was the greatest. Gain intensity was set just below saturating levels for the static (and no inhibitor in some cases) slide and those settings were used to image the remaining slides within a replicate for each protein of interest. The images shown are representative of the mean integrated fluorescence density for the protein indicated at each time point tested. ImageJ software was used to determine the integrated fluorescence density of the nucleus and cytoplasm of 10 to 15 cells per replicate. A single replicate consisted of a static, 15 min, 30 min, and in some cases a 60 min time point. Given that gain intensity differs between replicates, a normalization protocol was developed to allow for comparison across replicates with regard to a specific protein. Within a replicate, the changes in integrated fluorescence density values were determined relative to the mean integrated fluorescence density of the static (and no inhibitor in some cases) time point. Cell values for each time point within a replicate were averaged, yielding a single mean for each time point within the replicate. These time point mean values were then averaged across replicates and a statistical analysis was performed. For image presentation, the brightness and contrast of all p-cofilin and total cofilin images were increased by a value of 10 in the Zeiss software after analysis to enhance visual clarity. All images are orientated with the direction of FSS from the bottom to the top of the page.

Results

FSS-induced changes in cofilin phosphorylation

To address the question of cofilin involvement in early actin realignment, FSS-induced changes in cofilin activity were tracked by fluorescently labeling p-cofilin (serine-3) in confluent BAECs exposed to 15 dynes/cm^2 FSS for 15 and 30 mins. The intensity and spatial distribution of p-cofilin were different depending on the duration of FSS exposure (Figure 1). Under static conditions, p-cofilin was distributed throughout the cytoplasm and the nucleus, with nuclear staining being more intense, signifying a slightly higher concentration of cofilin phosphorylation (inactive) in the nucleus. Cytotoplasmic p-cofilin decreased in response to FSS by 43.56% at 15 mins ($n=9$, $p<0.0001$) and by 31.68% at 30 mins ($n=5$, $p=0.0036$) relative to static conditions. Nuclear p-cofilin increased in response to FSS by 39.00% at 15 mins ($n=9$, $p=0.0011$) and by 28.00% at 30 mins ($n=4$, $p=0.0253$) relative to static conditions, suggesting that FSS may induce cofilin phosphorylation (inactivation) in the nucleus. By 60 mins, p-cofilin had returned closer to control levels and differences were no longer significant. These results indicate that cofilin is responsive to FSS as illustrated by FSS-dependent changes in p-cofilin intensity and spatial distribution. Similar experiments to evaluate total cofilin with two different cofilin antibodies showed no FSS-induced differences relative to static conditions (Figure 1), indicating that cofilin is phosphorylated and inactivated in a particular location rather than FSS-inducing significant changes in p-cofilin movement or protein degradation. Secondary antibody only controls for both p-cofilin and total cofilin indicate that non-specific detection does not account for the staining patterns seen in both cases (data not shown). Similar results for p-cofilin and total-cofilin were also obtained with formaldehyde and Triton-X-100 fixed and permeabilized cells (data not shown). Because cofilin staining patterns of other cell types reported in the literature are different than what we observed in confluent endothelial cells, cofilin localization in sub-confluent BAECs was also determined. Total cofilin localization in sub-confluent BAECs was primarily cytoplasmic with little nuclear staining. Cytoplasmic total cofilin in sub-confluent BAECs was slightly elevated compared to confluent BAECs (data not shown). The staining pattern for p-cofilin in sub-confluent cells largely resembled p-cofilin staining in confluent endothelial cells (data not shown). These results suggest that confluent endothelial layers have different cofilin distributions than sub-confluent cells of many types.

Cofilin activity is required for FSS-induced actin realignment

In order to determine whether cofilin activity was required for FSS-induced actin realignment, two cofilin mutants were employed (Figure 2A). GFP-vinc was used as a transfection control and had no effect on FSS-induced actin realignment in the direction of FSS (Figure 2A, top panel). BAECs expressing the phosphorylation defective, constitutively active, serine-3-alanine (S3A) cofilin mutant formed atypical cortical actin bands at 30 mins, but failed to start elongating in the direct of FSS at 60 mins (Figure 2A, middle panel). BAECs expressing the phospho-mimic, constitutively inactive, serine-3-aspartic acid (S3D) cofilin mutant failed to form cortical actin bands at 30 mins and did not start elongating in the direction of FSS at 60 mins (Figure 2A, bottom panel). BAECs expressing either of the mutants have disorganized actin networks prior to the onset of FSS which persist through

FSS, with the S3D mutant resulting in highly atypical actin networks (Figure 2A). Both S3A and S3D-expressing BAECs had increased stress fibers relative to GFP-vinc expressing BAECs, with BAECs expressing S3D cofilin exhibiting the highest amount of stress fibers (Figure 2A). Western blots to detect p-cofilin (Figure 2B) and total cofilin (Figure 2C) in BAECs expressing S3A and S3D cofilin show similar cofilin levels in BAECs expressing the mutants as compared to GFP-vinc only cells. As shown in Figure 2B, specific p-cofilin bands were detected around 20.3 kD corresponding to the approximate molecular weight of cofilin, and around 27.9 kD corresponding to the approximate molecular weight of cofilin plus one ubiquitin. A large specific p-cofilin band around 12.5 kD was also detected, indicative of cofilin degradation (Figure 2B). Consistent with the total cofilin immunofluoresence data, total cofilin western blotting yielded very faint banding patterns similar to those detected in the p-cofilin blot (Figure 2C). Control cells and cells expressing either cofilin mutant exhibit specific banding patterns consistent with up to four ubiquitin chains indicative of increased targeting for protein degradation in cofilin mutant transfected BAECs (data not shown). Staining with a different total cofilin antibody resulted in darker staining of the 12.5 kD bands, but not darker staining of the intact or high molecular weight specific bands. Taken together, the results indicate that proper cofilin regulation is necessary for FSS-induced actin realignment and that cofilin is significantly degraded in confluent BAECs.

JNK and p38 involvement in FSS-induced cofilin phosphorylation

It has previously been reported that chemically inhibiting JNK with SP600125 and p38 with SB203580 blocked FSS-induced actin realignment in the direction of FSS (Mengistu et al., 2011, Azuma et al., 2001, Mengistu et al., 2012). Under static and FSS conditions, the roles of JNK and p38 in modulating cofilin phosphorylation were determined (Figure 3). Pretreatment of BAECs with SP600125 prior to FSS exposure resulted in significantly decreased cytoplasmic and nuclear p-cofilin. Cytoplasmic p-cofilin was decreased by 42.57% (n=4, p=0.0004) and nuclear p-cofilin was decreased by 45.00% (n=4, p=0.0012) relative to uninhibited BAECs at static conditions (Figure 3, middle panel). Upon FSS, SP600125-treated BAECs exhibited a 50.36% decrease in nuclear p-cofilin at 15 mins (n=3, p=0.0264) and a nuclear p-cofilin decrease of 40.63% (n=3, p=0.0745) that did not reach significance at 30 mins (Figure 3, middle panel) relative to uninhibited BAECs exposed to FSS for the same duration. BAECs treated with SP600125 and SB203580 vehicle did not differ from untreated cells at static conditions (data not shown). Pretreatment of BAECs with SB203580 prior to FSS exposure resulted in significantly decreased p-cofilin in the cytoplasm and the nucleus. Cytoplasmic p-cofilin decreased 38.61% (n=5, p=0.0009) and nuclear p-cofilin decreased 30.00% (n=5, p=0.0213) relative to uninhibited BAECs (Figure 3, bottom panel). p-cofilin levels in SB203580 pretreated cells were not significantly different from untreated cells after 15 and 30 mins of FSS (Figure 3, bottom panel). Continual exposure of BAECs to SP600125 during FSS did not differ from pre-treatment prior to FSS exposure (data not shown). Similar experiments investigating the affect of SP600125 on total cofilin localization showed no difference from untreated cells at the same time points (data not shown). Together these results imply that JNK and to a lesser extent p38 are involved in modulating cofilin activity in BAECs before and during FSS.

FSS-induced increased LIMK phosphorylation

Given that the majority of cofilin literature indicates that only dephoshorylated cofilin is capable of nuclear import under various cellular stressors (i.e. Pendleton et al., 2003, Iida et al., 1992), it is unlikely that p-cofilin is able to translocate to the nucleus. Therefore the major cofilin kinases, LIMK1/2, were analyzed for their roles in FSS-induced phosphorylation of cofilin in the nucleus. Under static conditions, pLIMK1/2 (threonine-508/505 – active) was distributed throughout the cytoplasm and the nucleus, with nuclear staining being slightly more intense (Figure 4a). Cytoplasmic pLIMK1/2 increased 46.00% (n=5, p=0.0003) at 15 mins and 54.00% (n=5, p=0.0348) at 30 mins of FSS relative to static conditions. Nuclear pLIMK1/2 increased 22.00% (n=5, p=0.0407) at 15 mins and 47.00% (n=5, p=0.0338) at 30 mins of FSS relative to static conditions. SP600125 was used to inhibit JNK and determine the role of JNK in mediating the effects on LIMK1/2 phosphorylation. Cells treated with SP600125 showed no significant differences in pLIMK1/2 relative to cells not treated with inhibitor at the same time point, suggesting that JNK is not upstream of pLIMK1/2 (Thr-508/505) (Figure 4a). These results indicate that pLIMK1/2 (Thr-508/505) is FSS responsive, providing a potential mechanism for the FSS-induced increase of p-cofilin in the nucleus, but this process does not appear to be mediated by JNK.

A second phosphorylation site on LIMK1L (serine-323), shown to be a p38-mediated phosphorylation site (Kobayashi et al., 2006), was also probed for FSS-induced activity changes. Under static conditions, pLIMK1L exhibited cytoplasmic and nuclear distribution (Figure 4b). Upon exposure to 15 dynes/cm^2 FSS for 15 and 30 mins, there were no apparent changes in pLIMK1L activity and spatial distribution (Figure 4b), suggesting that this phosphorylated form of LIMK1L is not responsive to FSS. These results, taken together with the p38 inhibitor results, indicate that p38 is likely not a major player in FSS-induced cofilin changes. Together with the pLIMK1/2 results, these results imply that only the conserved Thr-508/205 phosphorylation sites on LIMK1/2 are responsive to FSS.

Slingshot (serine-978) phosphorylation is not FSS-dependent

Because the changes seen in pLIMK1/2 localization cannot completely explain the changes in p-cofilin, FSS-induced localization changes in the major cofilin phosphatase, slingshot, were determined using antibodies specific for phosphorylation at serine-978 (pSSH), an established inhibitory phosphorylation site (Soosairajah et al., 2005). Prior to FSS exposure, pSSH is distributed fairly evenly throughout the nucleus and cytoplasm. Upon exposure to 15 dynes/cm^2 FSS for 15 and 30 mins, pSSH intensity did not significantly change in the nucleus or the cytoplasm, suggesting that slingshot activity is not responsive to FSS. In addition, when JNK was inhibited with SP600125 or p38 with SB203580, no significant differences were seen relative to the same time point without corresponding inhibitor (Figure 5a and b). In some cases, independent of FSS exposure or inhibitor treatment, a small subset of pSSH was localized to puncta along the cell membrane. Together these results indicate that slingshot phosphorylation at serine-978 is not responsive to FSS and that JNK and/or p38 is not involved in phosphorylating and inactivating slingshot under these conditions.

FSS-Induced VE-Cadherin and β-Catenin Localization at Cell-Cell Junctions

It has previously been shown that FSS decreases endothelial barrier permeability and strengthens the endothelial barrier (DePaola et al., 2001, Seebach et al., 2000). Therefore, we sought to determine the effects of actin realignment on barrier integrity by determining VE-cadherin, and β-catenin localization using the cofilin mutants and stress kinase inhibitors. Under static conditions, VE-cadherin staining was localized primarily to cell-cell contacts (Figure 6a, top panel – BAECs expressing GFP-vinc as a transfection control). Upon exposure to FSS, VE-cadherin staining became more regular at cell-cell contacts with fewer small gaps or breaks in the staining (Figure 6a, top panel), indicating an increase in apparent barrier integrity. This FSS-induced barrier tightening was absent from BAECs expressing either S3A (Figure 6a, middle panel) or S3D (Figure 6a, bottom panel) cofilin mutants as illustrated by large gaps (Figure 6a, arrowheads) or small breaks (Figure 6a, arrows) in VE-cadherin staining at cell-cell contacts. The gaps present in barrier staining were noticeably larger in BAECs expressing either cofilin mutant compared to GFP-Vinc. Similar results were obtained when cells were stained for β-catenin (Figure 6b). Taken together, these results imply that proper cofilin activity and actin alignment is required for enhancing cell-cell junctions during FSS.

In similar experiments, BAECs were treated with SP600125 (JNK inhibitor) or SB203580 (p38 inhibitor), exposed to 15 dynes/cm^2 FSS, and VE-cadherin was fluorescently stained. Again, under control conditions, VE-cadherin was localized to cell-cell contacts and apparent barrier integrity increased after FSS exposure (Figure 7a, top panel). BAECs treated with either SP600125 or SB203580 failed to exhibit the FSS-induced endothelial barrier tightening seen in the control experiments (Figure 7a, bottom panels), as evidenced by large gaps (Figure 7a, arrowheads) or small breaks (Figure 7a, arrows) in VE-cadherin staining. The gaps present in barrier staining were noticeably larger in BAECs treated with either inhibitor compared to uninhibited cells. Similar results were obtained when stained for β-catenin (Figure 7b). BAECs treated with SP600125 and SB203580 vehicle did not differ from untreated cells at static conditions (data not shown). Together, these results suggest that JNK and p38 are required to enhance endothelial barrier integrity during FSS.

Discussion

To our knowledge, this is the first report documenting that 15 dynes/cm^2 FSS causes a significant decrease in active cofilin in the nucleus and an increase in active cofilin in the cytoplasm without affecting total cofilin levels in either compartment. The lack of change in total cofilin indicates that FSS likely does not cause expression changes or alter protein degradation during FSS exposure up to 30 mins, but rather induces phosphorylation (activity) changes. The increase in active cofilin in the cytoplasm would allow for increased actin polymerization needed for cortical actin band formation and realignment of stress fibers in the direction of FSS. The increase in p-cofilin in the nucleus may be necessary to prevent cofilin from being exported back to the cytoplasm. These results help further our understanding of the atheroprotective nature of regions in the vasculature where blood flow is laminar with ECs exhibiting an elongated shape aligned in the direction of FSS (Langille and Adamson, 1981, Nerem et al., 1981). Our data also indicate that total cofilin in

confluent BAECs is predominantly nuclear, whereas in sub-confluent BAECs total cofilin is predominantly cytoplasmic, suggesting that confluent cells require less cytoplasmic cofilin than sub-confluent cells.

BAECs expressing either S3A or S3D cofilin failed to start elongating in the direction of FSS at 60 mins, and exhibited highly disorganized actin structures prior to the onset of FSS, suggesting that cofilin is essential for the process of FSS-induced actin realignment. The importance of cofilin activity regulation during FSS-induced actin realignment is illustrated in the fact that both cofilin mutants disrupt proper FSS-induced actin realignment. The increased stress fiber accumulation in the BAECs expressing S3D cofilin coincides with what would be more p-cofilin (inactive) leading to more stress fiber accumulation. S3A-expressing BAECs still form impaired cortical actin bands, again stressing the need for proper cofilin activity regulation during FSS. All cells (control or cofilin mutant) show high levels of cofilin degradation as assayed by western blotting, suggesting that confluent BAECs significantly degrade cofilin. Banding consistent with ubiquitination was observed in control and cofilin mutant cells, consistent with published evidence suggesting cofilin ubiquitination and proteosomal degradation (Yoo Y et al. 2010). Western blotting data for total cofilin was consistent with immunofluorescent imaging suggesting that cofilin is predominantly phosphorylated in BAECs.

Having established that the cofilin activity changes are regulated in part by FSS, the roles of stress kinases in this process were determined. Inhibition of JNK with SP600125 and inhibition of p38 with SB203580 significantly reduced the levels of p-cofilin in both the nucleus and the cytoplasm prior to the onset of FSS, establishing a role for JNK and p38 in modulating cofilin phosphorylation under static conditions. After the onset of FSS, we observed no additional affects of p38 inhibition, while JNK inhibition had significant continuing effects on nuclear p-cofilin but not cytoplasmic p-cofilin or nuclear or cytoplasmic total cofilin during FSS. An established p38-mediated phosphorylation site on LIMK1L (serine-323) (Kobayashi et al., 2006) was not FSS-responsive, suggesting that while p38 mediates FSS-induced actin remodeling, it is not due to LIMK1L phosphorylation at serine-323.

pLIMK1/2 (threonine-508/505) increased in the nucleus in response to 15 dynes/cm^2 FSS, ultimately leading to cofilin phosphorylation in the nucleus. Evidence from the literature supports the notion that both LIMK1 and LIMK2 possess a NLS and are capable of nuclear import and export (Yang and Mizuno, 1999, Goyal et al., 2005). These results suggest that cofilin can be phosphorylated in the nucleus, likely by pLIMK1/2. Despite the responsiveness of pLIMK1/2 to FSS, no effects of inhibiting JNK were seen. Although JNK and p38 have established roles in FSS-induced actin realignment and effects on cofilin phosphorylation, it appears that neither is acting through LIMK to facilitate these changes. The increase in cytoplasmic pLIMK1/2 in response to FSS is opposite to what we would expect given our data showing decreased cytoplasmic p-cofilin. Evidence from the literature indicates that FSS activates Rho/ROCK, leading to LIMK activation, as shown by in vitro cofilin phosphorylation, without distinguishing between nuclear and cytoplasmic compartments (Lin et al., 2003).

To examine the pattern of FSS-induced decreased p-cofilin in the cytoplasm, the responsiveness of the phosphatase slingshot to FSS was determined. Looking specifically at pSSH (serine-978), an established inhibitory phosphorylation site known to cause sequestration via 14-3-3 (Soosairajah et al., 2005), it was noted that overall pSSH levels do not change in response to FSS. Despite no FSS-induced pSSH protein level changes, puncta were evident in numerous cells. If SSH is the phosphatase responsible for cofilin dephosphorylation during FSS, JNK or p38 modulation of SSH activity is not mediated through serine-978 phosphorylation. It is also possible that these stress kinases do not modulate SSH activity. Other phosphatases may be necessary for transducing FSS stimuli. The exact mechanism leading to decreased cytoplasmic cofilin phosphorylation remains unclear.

Having determined that common cofilin kinases and phosphatases do not appear to be controlled by JNK or p38, we suspect that inhibiting JNK and p38 does not directly alter cofilin phosphorylation. Rather the effects of JNK and p38 on changes in cofilin phosphorylation may be due to altered cofilin accessibility instead of altered LIMK or SSH activity. Thus, the p-cofilin product would change, but not the covalent modifications that activate/inactivate the upstream kinases and/or phosphatases. One potential pathway known to regulate cofilin which has also been linked to FSS is the Rho/ROCK pathway, which leads to LIMK activation (Lin et al., 2003). Expression of dominant negative mutants of both Rho and ROCK disrupt FSS-induced actin realignment in BAECs (Li et al., 1999). Although this could explain the cofilin phosphorylation under FSS conditions, it does not appear to explain why blocking JNK or p38 decreases cofilin phosphorylation under control conditions. The cofilin regulation system is highly complex making it difficult to map out the signaling events downstream of FSS. It has been shown that SSH not only dephosphorylates (activates) cofilin, but is also capable of dephosphorylating (inactivating) LIMK, furthering the cell's ability to activate cofilin (Soosairajah et al., 2005, reviewed in Huang et al., 2006). An additional layer of complexity exists in that SSH is also enhanced by F-actin binding to enhance cofilin activation (Nagata-Ohashi et al., 2004, Soosairajah et al., 2005, reviewed in Huang et al., 2006). It is possible that the effect of inhibiting JNK and p38 is decreased during FSS, because of enhanced activation of SSH due to increased F-actin induced by the FSS, accompanied by SSH-induced LIMK inactivation and cofilin activation.

Since the cofilin mutants and stress kinase inhibitors disrupt FSS-induced actin realignment, they were used to determine how FSS-induced actin realignment affects barrier integrity. Cells expressing either S3A or S3D show numerous gaps and breaks in VE-cadherin or β-catenin staining at cell-cell junctions which were noticeably larger than GFP-vinc only cells, as do cells treated with stress kinase inhibitors. These results suggest that proper cofilin regulation and actin realignment are required to maintain and enhance cell-cell junctions during FSS, which is important for maintaining vascular barrier integrity. These results agree with published data showing that FSS decreases endothelial barrier permeability, preventing the transport of unwanted molecules across the endothelial layer (DePaola et al., 2001, Seebach et al., 2000).

Although we were unable to determine the link between cofilin and JNK or p38, it is clear that proper cofilin regulation, JNK activity, and p38 activity are required to maintain and

enhance endothelial cell junctions. It is reasonable to hypothesize that the central link is the actin cytoskeleton. Improper realignment of the actin cytoskeleton during FSS caused either by mutated cofilin or stress kinase inhibitors results in decreased barrier integrity. Actin associates with adherens junctions via β-catenin, which associates with the cytoplasmic domain of VE-cadherin (Tharakan et al. 2012). Therefore disrupting actin realignment during FSS has severe physiological outcomes in preventing FSS-induced barrier integrity, which would allow improper transport across the endothelial layer. These results emphasize the importance of FSS-induced actin realignment and maintenance of barrier integrity. Further support for the actin cytoskeleton in maintaining endothelial cell-cell junctions, was reported by Furman et al. (2007), where they showed that enabled/vasodilator-stimulated phosphoprotein (Ena/VASP) protein activity is required for normal stress fiber accumulation and cell-cell junction integrity (Furman et al., 2007).

In this report we document that FSS mediates changes in cofilin phosphorylation. FSS-induced increased p-cofilin in the nucleus is likely due to the need for actin function in the nucleus for elongation of the nucleus in the direction of FSS. pLIMK1/2 also increased in the nucleus after FSS exposure suggesting cofilin phosphorylation in the nucleus. Phosphorylation in the nucleus likely blocks export and could be a mechanism to retain cofilin in the nucleus. It is also clear that JNK activity induces cofilin phosphorylation in the nucleus, but this affect does not seem to be due to phosphorylation of LIMK1/2 or SSH, which did not change with SP600125 treatment. This suggests that JNK in some way enhances cofilin phosphorylation, but not through directly altering LIMK or SSH activity. Cofilin mutants were used to mimic specific states of cofilin phosphorylation, resulting in decreased correct actin realignment, regardless of whether there was a high level of inactive or of active cofilin. The cofilin mutants and stress kinase inhibitors decrease barrier integrity, illustrating the importance of correct actin realignment in endothelial barrier integrity during FSS.

Acknowledgments

Contract grant sponsor: NIH

Contract grant number: HL54269

The authors would like to thank Dr. Bryan Berger for the use of his lab’s electroporation equipment and continued collaborative efforts, Sara Lynn Nicole Farwell for critical manuscript review, and Maria Brace for assistance with figure preparation. Research from the LJL-K laboratory present herein was initiated with support from the Biosystems Dynamics Summer Institute, funded through an HHMI undergraduate education grant to Lehigh University. Ongoing research in the lab is funded by NIH grant award HL54269 to LJL-K.

References

Azuma N, Akasaka N, Kito H, Ikeda M, Gahtan V, Sasajima T, Sumpio BE. Role of p38 MAP kinase in endothelial cell alignment induced by fluid shear stress. Am J Physiol Heart Circ Physiol. 2001; 280:H189–H197. [PubMed: 11123233]

Bernard O. Lim kinases, regulators of actin dynamics. Int J Biochem Cell Biol. 2007; 39(6):1071–1076. [PubMed: 17188549]

Berstein BW, Bambrug JR. ADF/Cofilin: a functional node in cell biology. Trends in Cell Biology. 2010; 20(4):187–195. [PubMed: 20133134]

Bogoyevitch MA, Boehm I, Oakley A, Ketterman AJ, Barr R. Targeting the JNK MAPK cascade for inhibition: basic science and therapeutic potential. Biochimica et Biophysica Acta. 2004; 1697:89–101. [PubMed: 15023353]

Conway D, Schwartz MA. Lessons from the endothelial junctional mechanosensory complex. F1000 Biology Reports. 2012; 4:1. [PubMed: 22238515]

Côté MC, Lavoie JR, Houle F, Poirier A, Rousseau S, Huot J. Regulation of vascular endothelial growth factor-induced endothelial cell migration by LIM kinase 1-mediated phosphorylation of annexin-1. J Biol Chem. 2010; 285(11):8013–8021. [PubMed: 20061392]

Dejana E, Orsenigo F, Lampugnani MG. The role of adherens junctions and VE-cadherin in the control of vascular permeability. J Cell Sci. 2008; 121:2115–2122. [PubMed: 18565824]

DePaola N, Phelps JE, Florez L, Keese CR, Minnear FL, Giaever I, Vincent P. Electrical impedance of cultured endothelium under fluid flow. Ann Biomed Eng. 2001; 29:648–656. [PubMed: 11556721]

Furman C, Sieminski AL, Kwiatkawski AV, Rubinson DA, Vasile E, Bronson RT, Fässler R, Gertler FB. Ena/VASP is required for endothelial barrier function in vivo. J Cell Biol. 2007; 179(4):761–775. [PubMed: 17998398]

Goyal P, Pandey D, Behring A, Siess W. Inhibition of nuclear import of LIMK2 in endothelial cells by protein kinase C-dependent phosphorylation at Ser-283. J Biol Chem. 2005; 280(30):27569–27577. [PubMed: 15923181]

Gurniak CB, Perlas E, Witke W. The actin depolymerizing factor n-cofilin is essential for neuron tube morphogenesis and neural crest cell migration. Dev Biol. 2005; 278:231–241. [PubMed: 15649475]

Hahn C, Schwartz MA. Mechanotransduction in vascular physiology and atherogenesis. Nat Rev Mol Cell Biol. 2009; 10(1):53–62. [PubMed: 19197332]

Hahn C, Wang C, Orr AW, Coon BG, Schwartz MA. JNK2 promotes endothelial cell alignment under flow. PLoS ONE. 2011; 6(8):e24338.10.1371/journal.pone.0024338 [PubMed: 21909388]

Hamel M, Kanyi D, Cipolle MD, Lowe-Krentz LJ. Active stress kinases in proliferating endothelial cells associated with cytoskeletal structures. Endothelium. 2006; 13:157–170. [PubMed: 16840172]

Huang TY, DerMardirossian C, Bokoch GM. Cofilin phosphatases and regulation of actin dynamics. Curr Opin Cell Biol. 2006; 18:26–31. [PubMed: 16337782]

Iida K, Matsumoto S, Yahara I. The KKRKK sequence is involved in heat-shock-induced nuclear translocation of the 18-kDa actin-binding protein, cofilin. Cell Struct Funct. 1992; 17:39–46. [PubMed: 1586966]

Kadohama T, Akasaka N, Nishimura K, Hoshino Y, Sasajima T, Sumpio BE. p38 MAPK activation in endothelial cells is implicated in cell alignment and elongation induced by FSS. Endothelium. 2006; 13:43–50. [PubMed: 16885066]

Karderon D, Richardson WD, Markham AF, Smith AE. Sequence requirements for nuclear localization of simian virus 40 large-T antigen. Nature. 1984; 311:499–509.

Keezer SM, Ivie SE, Krutzsch HC, Tandle A, Libutti SK, Roberts DD. Angiogenesis inhibitors target the endothelial cell cytoskeleton through altered regulation of heat shock protein 27 and cofilin. Cancer Res. 2003; 63:6405–6412. [PubMed: 14559830]

Kobayashi M, Nishita M, Mishima T, Ohashi K, Mizuno K. MAPKAPK-2-mediated LIM-kinase activation is critical for VEGF-induced actin remodeling and cell migration. EMBO J. 2006; 25(4):713–26. [PubMed: 16456544]

Kumar S, Jiang MS, Adams JL, Lee JC. Pyridinylimidazole compound SB20580 inhibits the activity but not the activation of p38 mitogen-activated protein kinase. Biochema et Biophysica Res Comm. 1999; 263:825–831.

Langille BL, Adamson SL. Relationship between blood flow direction and endothelial cell orientation at arterial branch sites in rabbits and mice. Circ Res. 1981; 48:481–488. [PubMed: 7460219]

Lin MC, Galletta BJ, Sept D, Cooper JA. Overlapping and distinct functions for cofilin, coronin, and Aip1 in actin dynamics in vivo. J Cell Sci. 2010; 123:1329–1342. [PubMed: 20332110]

Lin T, Zeng L, Liu Y, DeFea K, Schwartz MA, Chien S, Shyy JA. Rho-ROCK-LIMK-Cofilin pathway regulates shear stress activation of sterol regulatory element binding proteins. Circ Res. 2003; 92:1296–1304. [PubMed: 12775580]

Li S, Chen BP, Azuma N, Hu YL, Wu SZ, Sumpio BE, Shyy JY, Chien S. Distinct roles for the small GTPases Cdc42 and Rho in endothelial responses to shear stress. J Clin Invest. 1999; 103:1141–1150. [PubMed: 10207166]

Malek AM, Izumo S. Mechanism of endothelial cell shape change and cytoskeletal remodeling in response to fluid shear stress. J Cell Sci. 1996; 109:713–726. [PubMed: 8718663]

Mengistu M, Brotzman H, Ghadiali S, Lowe-Krentz LJ. Fluid shear stress-induced JNK activity leads to actin remodeling for cell alignment. J Cell Physiol. 2011; 226(1):110–121. [PubMed: 20626006]

Mengistu, M.; Slee, JB.; Lowe-Krentz, LJ. Stressed Out and Actin Up: stress-activated protein kinase regulation of actin remodeling directs endothelial cell morphology and migration. In: Consuelas, VA.; Minas, DJ., editors. Actin: Structure, Functions, and Disease. New York: Nova Science Publishers; 2012. p. 177-205.

Nagata-Ohashi K, Ohta Y, Goto K, Chiba S, Mori R, Nishita M, Ohashi K, Kousaka K, Iwamatsu A, Niwa R, Uemura T, Mizuno K. A pathway of neuregulin-induced activation of cofilin-phosphatase slingshot and cofilin in lamellipodia. J Cell Biol. 2004; 165:465–471. [PubMed: 15159416]

Nerem RM, Levesque MJ, Cornhill JF. Vascular endothelial morphology as an indicator of the pattern of blood flow. J Biomech Eng. 1981; 103:172–176. [PubMed: 7278195]

Nishida E, Maekawa S, Sakai H. Cofilin, a protein in porcine brain that binds to actin filaments and inhibits their interaction with myosin and tropomyosine. Biochemistry. 1984; 23:5307–5313. [PubMed: 6509022]

Noria S, Xu F, McCue S, Jones M, Gotlieb AI, Langille BL. Assembly and reorientation of stress fibers drives morphological changes to endothelial cells exposed to shear stress. Am J Pathol April. 2004; 164(4):1211–1223.

Ohura N, Yamamoto K, Ichioka S, Sokabe T, Nakatsuka H, Baba A. Global analysis of shear stress-responsive genes in vascular endothelial cells. J Atheroscler Thromb. 2003; 10:304–313. [PubMed: 14718748]

Osborn EA, Rabodzey A, Dewey CF Jr, Hartwig JH. Endothelial actin cytoskeleton remodeling during mechanostimulation with fluid shear stress. Am J Physiol Cell Physiol. 2006; 290:C444–52. [PubMed: 16176968]

Pederson T. As functional nuclear actin comes into view, is it globular, filamentous, or both? J Cell Biol. 2008; 180:1061–1064. [PubMed: 18347069]

Pendleton A, Pope B, Weeds A, Koffer A. Latrunculin B or ATP depletion induces cofilin-dependent translocation of actin into nuclei of mast cells. J Biol Chem. 2003; 278(16):14394–14400. [PubMed: 12566455]

Rüegg J, Holsboer F, Turck C, Rein T. Cofilin 1 is revealed as an inhibitor of glucocorticoid receptor by analysis of hormone-resistant cells. Mol Cell Biol Nov. 2004; 24(21):9371–82.

Seebach J, Dieterich P, Luo F, Schillers H, Vestweber D, Oberleithner H, Gall HJ, Schnittler HJ. Endothelial barrier function under laminar fluid shear stress. Lab Invest. 2000; 80(12):1819–1831. [PubMed: 11140695]

Soosairajah J, Mairi S, Wiggan O, Sarmiere P, Moussi N, Sarcevic B, Sampath R, Bamburg JR, Bernard O. Interplay between components of a novel LIM kinase-slingshot phosphatase complex regulates cofilin. EMBO J. 2005; 24:473–486. [PubMed: 15660133]

Suurna MV, Ashworth SL, Hosford M, Sandoval RM, Wean SE, Shah BM, Bamburg JR, Molitoris BA. Cofilin mediates ATP depletion-induced endothelial cell actin alterations. Am J Physiol Renal Physiol. 2006; 290:F1398–1407. [PubMed: 16434575]

Tharakan B, Hellman J, Sawant DA, Tinsley JH, Parrish AR, Hunter FA, Smythe WR, Childs EW. β-catenin in the regulation of microvascular endothelial cell hyperpermeability. Shock. 2012 Mar; 37(3):306–311. [PubMed: 22089197]

Tzima E, Irani-Tehrani M, Kiosses WB, Dejana E, Schultz DA, Engelhardt B, Cao G, DeLisser H, Schwartz MA. A mechanosensory complex that mediates the endothelial cell response to fluid shear stress. Nature. 2005; 437:426–431. [PubMed: 16163360]

Vincent PA, Xiao K, Buckley KM, Kowalczyk AP. VE-cadherin: adhesion at arm's length. Am J Physiol Cell Physiol. 2004; 286:C987–97. [PubMed: 15075197]

Won KJ, Park SH, Park T, Lee CK, Lee HM, Choi WS, Kim SJ, Park PJ, Jang HK, Kim SH, Kim B. Cofilin Phosphorylation mediates proliferation in response to platelet-derived growth factor-BB in rat aortic smooth muscle cells. J Pharmacol Sci. 2008; 108:372–379. [PubMed: 19023180]

Yalcin HC, Perry SF, Ghadiali SN. Influence of airway diameter and cell confluence on epithelial cell injury in an in-vitro model of airway reopening. J Appl Physiol. 2007; 103:1796–1807. [PubMed: 17673567]

Yamamoto K, Ando J. New molecular mechanisms for cardiovascular disease: Blood flow sensing mechanism in vascular endothelial cells. J Pharmacol Sci. 2011; 116:323–331. [PubMed: 21757846]

Yang N, Mizuno K. Nuclear export of LIM-kinase 1, mediated by two leucine-rich nuclear export signals within the PDZ domain. Biochem J. 1999; 338:793–798. [PubMed: 10051454]

Yoo Y, Ho HJ, Wang C, Guan JL. Tyrosine phosphorylation of cofilin at Y68 by v-src leads to its degradation through ubiquitin-proteasome pathway. Oncogene. 2010; 14;29(2):263–272.

Zheng B, Han M, Bernier M, Wen JK. Nuclear actin and actin-binding proteins in the regulation of transcription and gene expression. FEBS J. 2009; 276:2669–2685. [PubMed: 19459931]

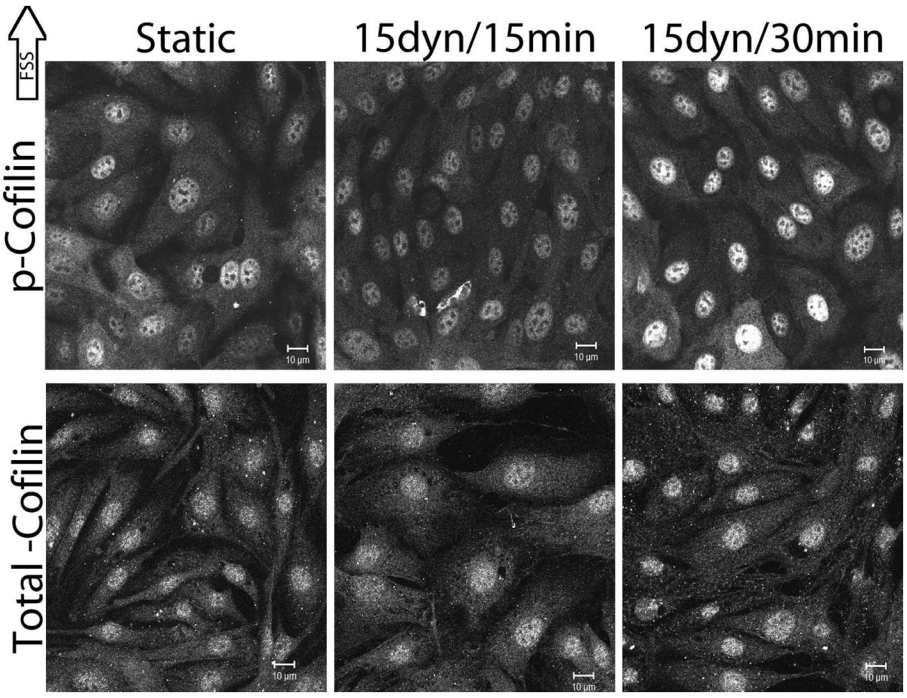

Figure 1.

FFS-induced changes in cofilin phosphorylation.

Confluent monolayers of BAECs were exposed to 15dynes/cm^2 FSS for 15 and 30 mins. BAECs were labeled with antibodies against p-cofilin (top panel) or total cofilin (bottom panel) (Santa Cruz Biotechnology). Gain intensity was set just below saturating levels for the static p-cofilin and total cofilin separately and those settings were used to image the remaining slides within the replicate for each protein. Image analysis was performed as described in the methods. Images shown are representative of at least 3 replicates. Scale bars = 10μm.

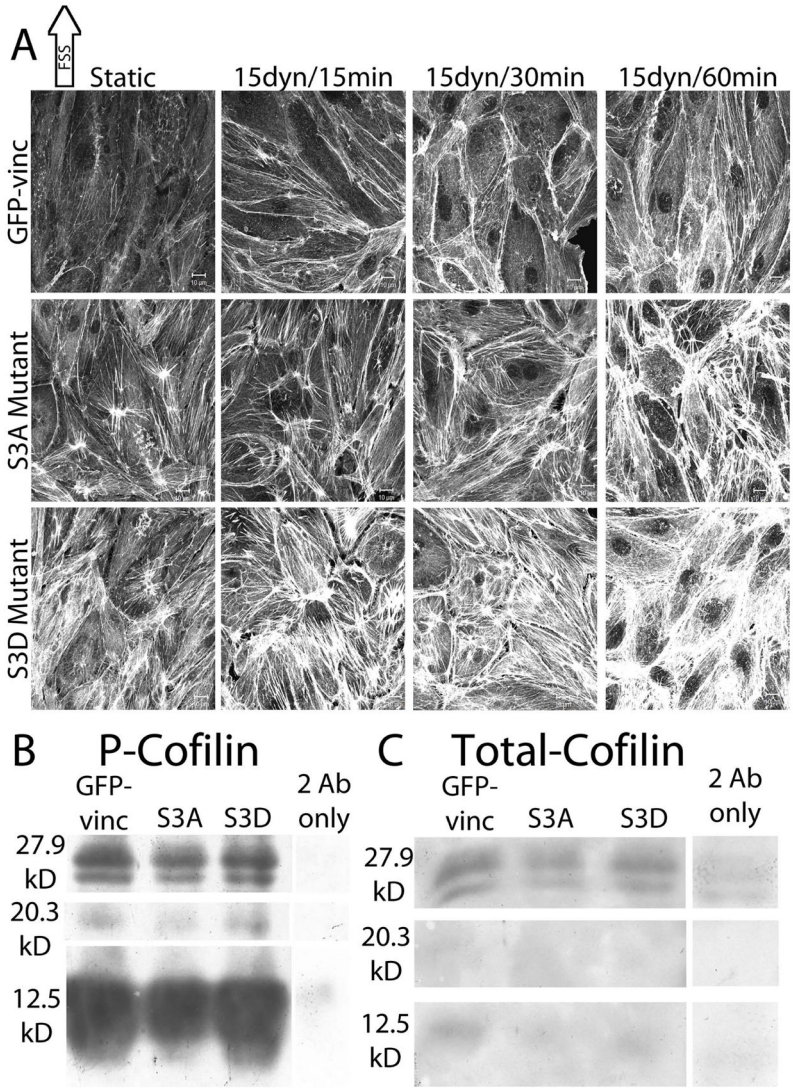

Figure 2.

The effect of cofilin activity on FSS-induced actin realignment

BAECs were electroporated with 20μg/ml of either S3A or S3D cofilin constructs in combination with GFP-vinc as a fluorescent marker of transfection efficiency as described in the methods. BAECs expressing the mutant constructs were exposed to 15 dynes/cm^2 FSS for 15, 30, and 60 mins and labeled for actin stress fibers using TRITC-phalloidin. The images shown are representative of 10 repeats. [A] Top panel, BAECs expressing GFP-vinc alone showing FSS-induced actin realignment. Middle panel, BAECs expressing S3A cofilin showing impaired actin realignment during FSS. Bottom panel, BAECs expressing S3D cofilin showing impaired actin realignment during FSS. Scale bars = 10μm. [B, C] BAECs were electroporated with GFP-vinc, S3A cofilin, or S3D cofilin as indicated. Whole cell lysates harvested 24–48 hours post transfection were immunoblotted with anti-p-cofilin [B] or anti-total cofilin [C] antibodies. Corresponding secondary antibody only controls (2 Ab only) were also performed for both p-cofilin [B] and total cofilin [C]. Molecular weights

of the bands were calculated based on Rf values created from the markers are indicated on the left.

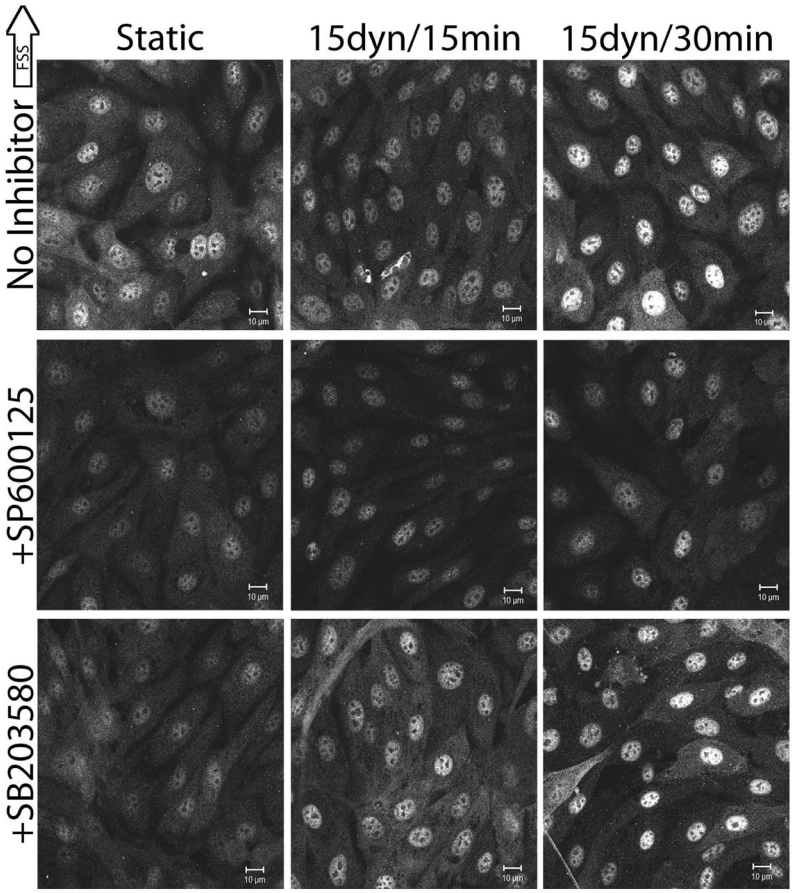

Figure 3.

The roles of JNK and p38 in FSS-induced cofilin phosphorylation

Confluent monolayers of BAECs were treated with SP600125 (JNK inhibitor) or SB203580 (p38 inhibitor) for 1 hr prior to FSS exposure. Following inhibitor incubation, BAECs were exposed to 15 dynes/cm^2 FSS for 15 and 30 mins and labeled with antibodies against p-cofilin. Image analysis was performed as described in the methods. The images shown are representative of at least 3 replicates. Top panel, uninhibited BAECs. Middle panel, SP600125-treated BAECs. Bottom panel, SB203580-treated BAECs. Scale bars = 10μm.

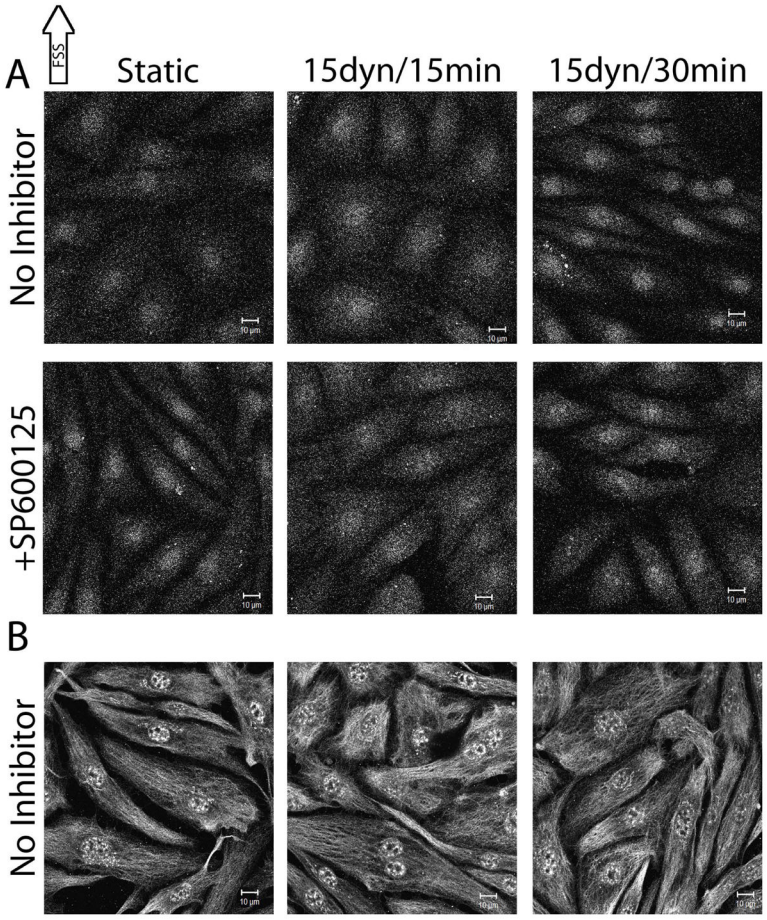

Figure 4.

FFS-induced changes in LIMK phosphorylation

Confluent monolayers of BAECs were exposed to 15dynes/cm^2 FSS for 15 and 30 mins and labeled with antibodies against pLIMK1/2 (threonine-508/505) [A] or pLIMK1L (serine-323) [B]. Image analysis was performed as described in the methods. The images shown are representative of at least 4 replicates. [A]. Top panel, uninhibited BAECs. Bottom panel, SP600125-treated BAECs. [B]. Uninhibited BAECs. Scale bars = 10μm.

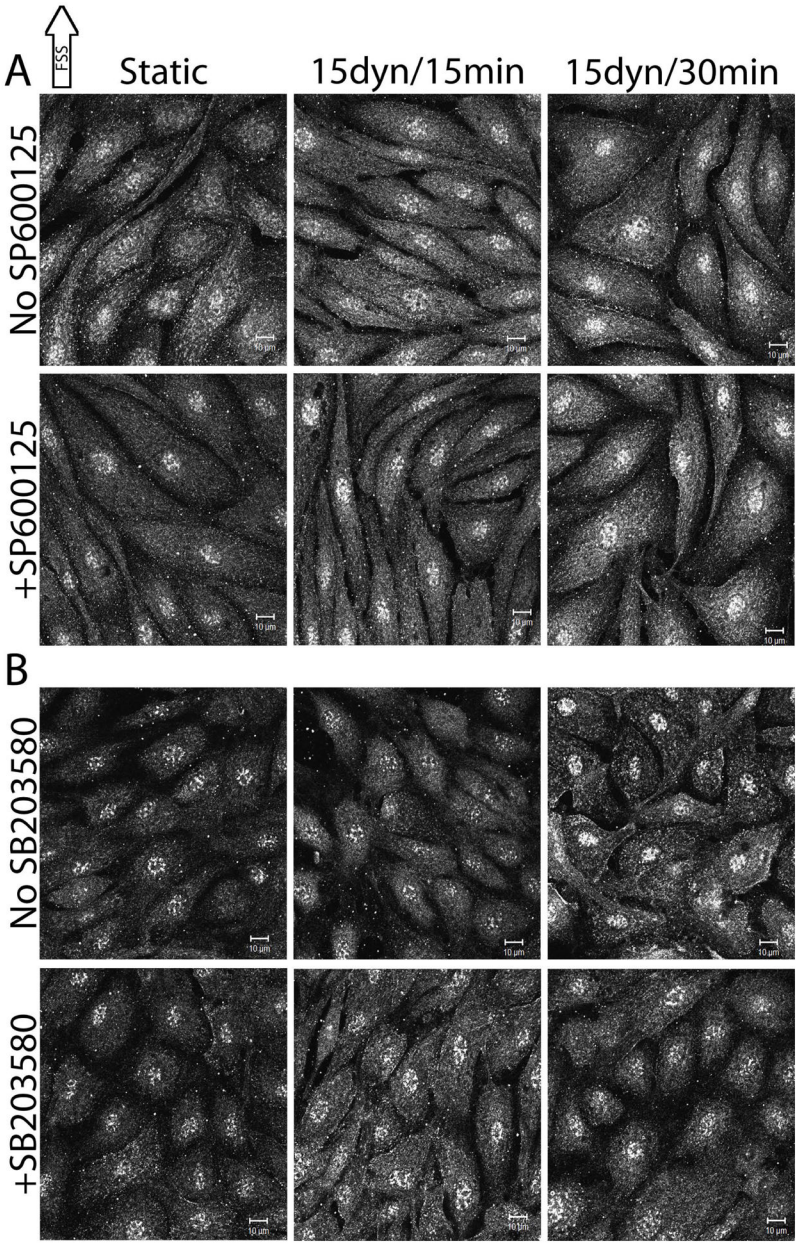

Figure 5.

FSS-induced changes in SSH phosphorylation

Confluent monolayers of BAECs were exposed to 15dynes/cm^2 FSS for 15 and 30 mins and labeled with antibodies against pSSH (serine- 978). Image analysis was performed as described in the methods. The images shown are representative of at least 3 repeats. [A] SP600126-treated BAECs. [B] SB203580-treated BAECs. Scale bars = 10μm.

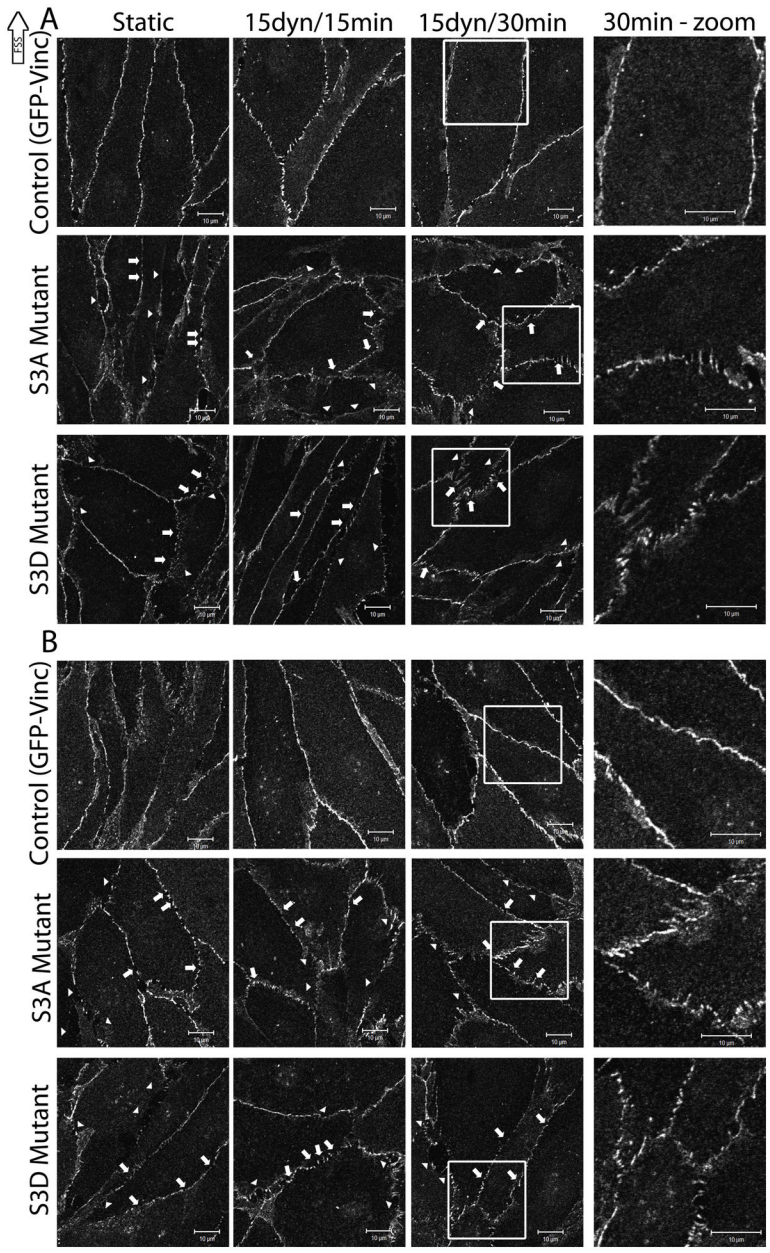

Figure 6.

The role of cofilin in FSS-induced barrier staining

BAECs were electroporated with 20μg/ml of either S3A or S3D cofilin constructs in combination with GFP-vinc as a fluorescent marker of transfection efficiency as described in the methods. BAECs expressing the mutant constructs were exposed to 15 dynes/cm^2 FSS for 15 and 30mins and labeled using antibodies against VE-cadherin [A] or β-catenin [B]. The images shown are representative of 3 repeats. In both A and B, the top panel images are expressing GFP-vinc alone, the middle panel images are BAECs expressing S3A and GFP-Vinc, and the bottom panel images are BAECs expressing S3D and GFP-vinc. The three left columns are magnified 2X the original. The rightmost column is magnified 4X the original

and highlights the boxed area in the column immediately to the left. Arrows point to small breaks in staining. Arrowheads point to large gaps in staining. Scale bars = 10μm.

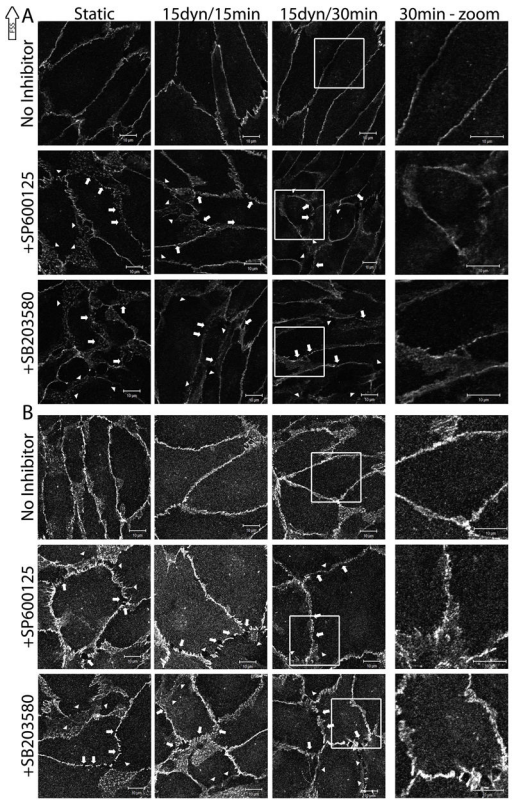

Figure 7.

The role of JNK and p38 activity in FSS-induced barrier staining

Confluent monolayers of BAECs were treated with SP600125 (JNK inhibitor) or SB203580 (p38 inhibitor) for 1 hr prior to FSS exposure. Following inhibitor incubation, BAECs were exposed to 15 dynes/cm^2 FSS for 15 and 30 mins and labeled with antibodies for VE-cadherin [A] or β-catenin [B]. The images shown are representative of the trends which have been identified through at least 2 repeats. In both A and B, the top panel images are expressing GFP-vinc alone, the middle panel images are BAECs expressing S3A and GFP-vinc, and the bottom panel images are BAECs expressing S3D and GFP-vinc. The three left columns are magnified 2X the original. The rightmost column is magnified 4X the original and highlights the boxed area in the column immediately to the left. Arrows point to small breaks in staining. Arrowheads point to large gaps in staining. Scale bars = 10μm.